75th International Astronautical Congress (IAC), Milan, Italy, 14-18 October 2024.

IAC-24-A6,IPB,19,x86639

Application of active feedback control for investigation of debris mitigation strategies on a density-based model of the population evolution

Martina Rusconi[a,*], **Lorenzo Giudici**[a], **Camilla Colombo**[a]

[a] *Department of Aerospace Science and Technology, Politecnico di Milano, Via La Masa 34, 20156, Milan, Italy. martina.rusconi@polimi.it, lorenzo1.giudici@polimi.it, camilla.colombo@polimi.it*
[*]Corresponding author: martina.rusconi@polimi.it

Abstract

The population of objects in space faced an unforeseeable growth in the last decades. Therefore, it is now imperative to reiterate the debris mitigation guidelines and reconsider the approach to the debris proliferation problem. Different counteractions are available to deal with the situation. However, how to efficiently combine and apply these methods for sustainable use of the space environment is still an open question. To respond to this need, the GREEN SPECIES project, funded by a consolidator grant of the European Research Council, will develop a controlled model of the space debris population to define optimal mitigation policies. In its current version, the system exploits a statistical model in which debris and intact objects move in a one-dimensional domain in orbital radius and binned in spherical shells. The evolution of the environment is modelled in terms of the objects' density dynamics. The system includes the effect of atmospheric drag, sources as launches and in-orbit fragmentations, and artificial sink mechanisms such as post mission disposals and active debris removals. The resulting set of ordinary differential equations is integrated with a state-dependent linear feedback controller to tune different inputs and reach a predefined target. The novel appraoch exploits the benefits of control techniques to investigate the effectiveness of diversified rules in space and time to mitigate the debris proliferation and its risk to missions in low Earth orbit.
Keywords: Debris, Complex system, Control, Mitigation.

Nomenclature

A [$m^{-6}s^{-1}$]	State weight matrix
a [m]	Semi-major axis
B [variable]	Control weight matrix
C [$m_{-3}s^{-1}$]	Disturbance matrix
D [-]	Gain matrix
e [m^{-3}]	State error
e [-]	Eccentricity
F [s^{-1}]	State matrix
G [variable]	Control matrix
J [-]	Cost function
N [-]	Number of items
n [m^{-3}]	Spatial density
P_c [-]	Collision probability
$\dot{n}$ [$m^{-3}s^{-1}$]	Density rate
r [m]	Orbital radius
S [m^{-6}]	Gain matrix
S [m^2]	Surface
t [s]	Time
V [m^3]	Volume
v_r [ms^{-2}]	Radial velocity
W [-]	Gain matrix
x [m^{-3}]	State
α [-]	ADR percentage
λ [-]	PMD compliance
σ [m^2]	Cross-sectional area

Acronym/Abbreviations

ADR	Active Debris Removal
LEO	Low Earth Orbit
MPC	Model Predictive Control
PD	Proportional Derivative
PMD	Post Mission Disposal
SDRE	State-Dependent Riccati Equation
SDDRE	State-Dependent Differential Riccati Equation

1. Introduction

At the beginning of the space era, Earth's orbital environment appeared as an infinite resource. Nowadays and in the future, all the new missions and actors that want to access space will have to face the debris problem. The number of derelict objects orbiting Earth is increasingly growing [1]. Each of them, be it a large, disposed satellite or a very small fragment, poses a serious risk to every newly launched spacecraft, and each newly launched spacecraft is by itself a threat to others in case of in-orbit collisions that would aliment the growing debris population. Since the first approach to the problem at the end of the 20th century, several studies have been conducted exploiting observational data and on-ground

tests, to understand and predict the evolution of this accumulation of objects (e.g. [2], [3], [4]). As a result of this campaign, different counteractions have been formulated to mitigate the problem, such as widespread implementation of Post-Mission Disposal (PMD) options or passivation of items with residual stored energy. These actions came in the form of mission design guidelines in 2002 [5]. Afterwards, the scientific community continued to analyse the current and estimated future scenarios of the space environment population, developing evolutionary models progressively more advanced and accurate and reporting the results of their investigations on a yearly basis [1]. Recent results clearly show that the present approach to deal with the debris proliferation problem is insufficient and update of the mitigation strategy is a pressing necessity. Some new actions have already been taken by the European Space Agency (ESA), as the definition of internal mitigation guidelines and policy [6].

It is not the first time that humanity has to face such an exponentially growing environmental stressor. Since industrialisation began, carbon dioxide concentration in the atmosphere started to grow progressively faster, causing today's climate change problem. Debris proliferation is behaving similarly to the trend of CO_2 atmospheric concentration throughout the years. The latter is a long and widely studied phenomenon in which looping between analysis of Earth's environmental data and update of intergovernmental instructions has been going on for decades. The scientific community for climate change developed models to investigate the physical and socio-economical effects of CO_2 excessive emissions and its mitigation measures, the integrated assessment models, one of the most popular being the DICE model [7]. A visual interpretation of the common approach of looping between analysis of observational data and scientific theory and the definition of a reaction strategy towards sustainability is given in Fig. 1, for both CO_2 mitigation in climate change economics and debris mitigation in the space field, a process that began with the rise of the space era and is getting faster every decade. The GREEN SPECIES project, funded by the European Research Council through a consolidator grant, aims at developing a "Robust control of the space debris population to define optimal policies and an economic revenue model for sustainable development of space activities". Core activity of the project is the development of an actively controlled model of the evolution of the population of objects in space, which is a quite new field of investigation. The integrated system will enter the loop in Fig. 1 and provide the space scientific experts directly with an ideal strategy to face efficiently the debris proliferation and ease guidelines definition. A common approach to the problem includes the control of a simplified statistical model with reduced number of dimensions. In literature there are many examples of statistical models to capture the evolution of the number of objects in a binned domain or Particle-In-a-Box (PIB) models. Talent was one of the first to exploit a PIB approach for debris environment analysis [2], the FADE model was developed at the University of Southampton [8], while an Italian example is the STAT system by Rossi et al. [3]. These representations have been used throughout the years to investigate the effect of the different parameters with which humans can act on the debris environment, such as deployment rate of objects in [9] and [10]. Lately, their integration with an active control is gaining popularity. In [11] the authors apply an adaptive strategy to tune the yearly rate of Active Debris Removals (ADR) within the model CASCADE for the one-dimensional propagation of the number of objects orbiting Earth in altitude shells. MISSD by Somma et al. [12] exploited a similar system of first-order, non-linear, ordinary differential equations to describe the rate of change of the number or density of objects in space under the effect of source and sink effects. A feedback controller is applied to adjust the ADR rate based on proportional, linear or quadratic control logic in the state error. More recently, a Proportional-Derivative (PD) controller and a nonlinear Model Predictive Control (MPC) approach have been used on the MOCAT-SSEM [13], developed at MIT, where space objects move and interact similarly to Somma's work. In that study, the controllers act on each family of objects in orbit to define suitable launch and ADR rates to minimise a defined cost objective. Following the preliminary work described in [14], the statistical model developed and used in this work accounts for the evolution of the density of objects per altitude shell under the effect of drag, launches, post-mission disposal, active-debris removals and in-orbit collisions. A linear feedback controller acts on the system to tune the inputs and minimise a quadratic cost function.

The paper is structured as follows: first each effect modelled in the analysis is described and the control logic derived in Sections 2 and 3, then the system is applied to study cases with common target and different control strategies in Section 4, and finally in Section 5 the main conclusions with considerations on future work are summarised.

2. The debris model

As clear from the previously cited works, a statistical model limited in size is beneficial from a control system standpoint. It would be too computationally expensive and often unfeasible to apply modern robust control techniques to highly nonlinear multi-dimensional systems.

Consequently, the novel integration of a density-based approach and an active control is exploited to represent the spatial evolution of the objects' distribution, as previously done in [14]. The objects around Earth are considered as a continuous flow that moves in a one-dimensional space under the action of environmental effects, sources and sinks. A graphical representation of

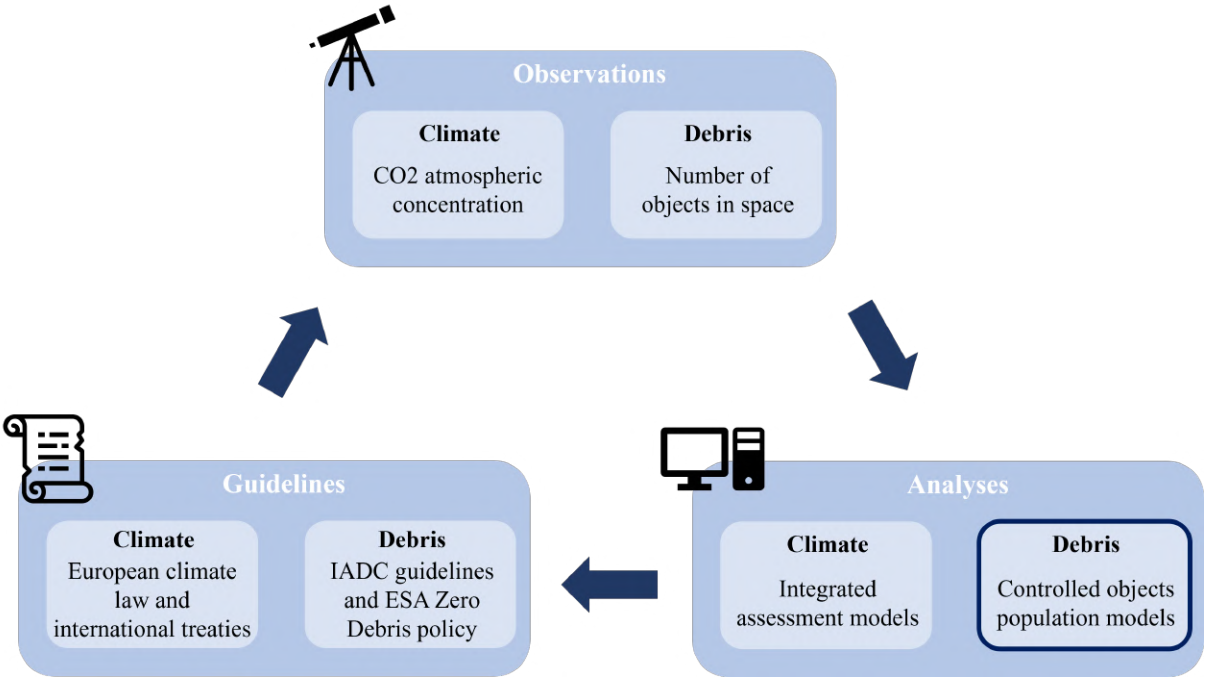

Fig. 1. Scientific approach loop applied over time to study the climate change and the debris situation. From observations of empirical data models are reconstructed, the results of the analyses are then interpreted by the scientific community to support definition of guidelines. These will change the observed environment and will be updated to adapt to the changed situation.

the model is given in Fig. 2. The lower Earth orbital re-

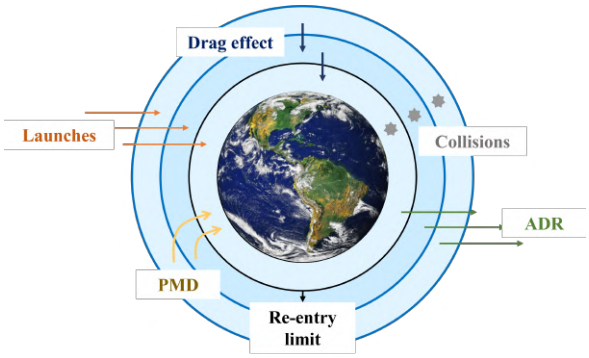

Fig. 2. Graphical representation of the model. The domain is divided in spherical shells and in each of them the density of the number of objects is affected by atmospheric drag, launches, in-orbit collisions, and PMD and ADR above the re-entry limiting radius.

gion between 200 km and 2000 km is divided in spherical shells of constant width of 50 km and the only spatial dimension considered is the orbital radius that identifies each bin. Starting from a reference population of intact objects and debris fragments in orbit, the spatial density $n(r)$ in each shell is computed from the orbital parameters of each item (semi-major axis a, eccentricity e and orbital radius r) with Kessler's derivation in Equation 1 [15]. The contribution of each element in a shell is weighted on the time spent by the same in an infinitesimal volume around the central radius of the considered bin, and the overall density at r obtained summing the contributions.

$$n_j(r) = \frac{1}{4\pi^2 r a^2 \sqrt{e^2 - (\frac{r}{a} - 1)^2}} \qquad n(r) = \Sigma_{j=1}^{N_f} n_j(r) \tag{1}$$

With this definition, information on the orbit's shape of the objects is lost, and they are considered moving along circular paths. The dynamics of the initial profile is computed enforcing conservation in time and space of the overall number of objects of the system through the integral form of a continuity Equation 2 in each volume V, where S is the boundary surface of the shell, v_r the radial velocity associated to r in that shell, and $\dot{n}^+$ and $\dot{n}^-$ are sources and sinks density rates.

$$\frac{dn}{dt} = \frac{1}{V}\left[-\int_S (v_r n) dS + \int_V \dot{n}^+ - \int_V \dot{n}^-\right] \tag{2}$$

This density-based approach is a novel approach used for propagation of populations of objects and that has been also adopted for space debris applications. McInnes proposed a density formulation of the distribution of nanosatellites constellations [16], Letizia et al. developed the CiELO suite for debris clouds analytical propagation in time and orbital radius [17]. Then, several works performed at Politecnico di Milano extended the model to describe the evolution of the overall debris population [18] and to account for feedback effect of in-orbit fragmentations on the background objects [19]. More recently, the Starling 2.0 and COMETA suites

have been developed at Politecnico di Milano to simulate the evolution of debris clouds alone or within a populated environment, exploiting the density formulation for the smaller particles in a up to 7D phase space and under any orbital regime [20][4].
In the current formulation of the model, Equation 2 is propagated in time, applying a finite volume method with respect to the binned environment, similarly to the work in [4]. In Fig. 2 all the contributions that affect the evolution of the density in each shell are represented. The initial population is divided in two species: intact objects and fragments. The former include payloads, rocket bodies and large debris whose sectional area is above 1 m^2 and no manoeuvrability is assumed, the latter include all the smaller debris. A more detailed division will be considered in future work based on objects' type and physical properties.
For each family, the first contribution in Equation 2 models the stretching of a shell volume due to environmental effects. Atmospheric drag is the major perturbation acting in LEO and, when looking at the long-term effects, the J_2 perturbation acting on shorter time scales can be neglected. So the evolution of the volume bin in time, identified in the orbital radius one-dimensional radial velocity term v_r in Equation 2, is described through the King-Hele drag force model proposed in [21]. The atmospheric density is modelled as a sum of exponential functions and the solar flux effect is included through a time-varying sinusoidal function, following the approach in [4].
The sources and sinks considered in the analysis are: launch traffic, PMD operations, ADR and collisions between two intact objects in the same shell and between intact objects and fragments in a volume. The extended dynamical system with all the contributions in the i^{th} shell, delimited by radii r_{lower} and r_{upper}, is given in Equation 3, for both species in all the N_s shells.

$$\begin{cases} \frac{dn_{obj_i}}{dt} = & \frac{1}{V}\Bigg[-\Big(4\pi n_{obj_{i+1}} v_{r_{i+1}} r^2_{i_{upper}} \\ & -4\pi n_{obj_i} v_{r_i} r^2_{i_{lower}}\Big) \\ & +\frac{N_{i_L}}{1year} - \lambda \int_{V_{t_L}} \frac{\dot{n}_{i_L}(t_L)}{1year} \\ & -\alpha \frac{N_{i_{ADR}}}{1year} - 2P_{c_{i_{obj-obj}}}\Bigg] \\ \vdots & \text{for} \quad i = 1, ..., N_s \\ \frac{dn_{frag_i}}{dt} = & \frac{1}{V}\Bigg[-\Big(4\pi n_{frag_{i+1}} v_{r_{i+1}} r^2_{i_{upper}} \\ & -4\pi n_{frag_i} v_{r_i} r^2_{i_{lower}}\Big) \\ & -P_{c_{obj-frag}} + P_{c_{obj-frag}} N_{nc} \\ & +P_{c_{i_{obj-obj}}} N_c\Bigg] \\ \vdots & \text{for} \quad i = 1, ..., N_s \end{cases} \tag{3}$$

An historical repetition of the launch traffic of the 5 years prior to the initial epoch of the simulations is considered, similar to the analysis performed in [22][4], under the assumptions that the future space activities will not differ much from the recent ones. For each shell, the number of objects deployed in a year is retrieved and a constant yearly launch rate applied in terms of density deposition rate $\frac{N_{i_L}}{1year}$.
The post-mission disposals are based on the launch traffic implemented, similarly to [14]. Given a constraint in terms of re-entry time of the disposed objects, the effect is active only on the shells above the minimum altitude satisfying this requirement, the re-entry radius limit in Fig. 2. As an example, to satisfy the 25 years rule [5] only spent objects in the shells above 630 km are disposed below this limit, according to the King-Hele drag model. At each time instant t the number of objects launched at a previous time t_L and that are now at end of life in the current volume shell is retrieved as in the third term of Equation 3: $\int_{V_{t_L}} \frac{\dot{n}_{i_L}(t_L)}{1year}$, where t_L is defined as $t_L = t - t_{L->PMD}$ with $t_{L->PMD}$ time between launch and PMD and where the density rate of launches at time t_L is integrated over the shell volume stretched back in time up to t_L. A percentage λ of these objects eligible for disposal is instantaneously removed and placed in the first shell completely below the re-entry limit.
It is difficult to make assumptions on the future of ADR, its application is beginning nowadays and no historical data are available for this effect. So, when the ADR rate is not a control input, as a first assumption a constant yearly effect in each shell is considered as $\alpha \frac{N_{i_{ADR}}}{1year}$, in terms of a fixed percentage α of a maximum number of removals per year in each shell. In future work, more accurate time-varying profiles could be easily included in the model. Moreover, similarly to the PMD approach, also the removals are considered applied only above the limiting radius in Fig. 2.
According to Kessler's theory proposed in [23] and as demonstrated by recent investigations, on-orbit collisions are the major contribution to debris proliferation, a phenomenon that is growing and self-sustaining. In the model collisions are included adopting the approach in [12]. Only impacts between two intact objects or between fragments and intact object are modelled, with the strong assumption that all the generated particles are injected in the shell of the fragmentation. The collision probability in a shell, P_c in Equation 3, is defined through the kinetic theory of gases as in Equation 4, whose definition can be found in [15]. In Equation 4 σ_{obj} is the average cross-sectional area of the impacting object, which is assumed much larger than the impacting fragments' area. It is obtained averaging the $\sigma_{i_{obj}}$ values of each object in the initial population and kept fixed.

$$\begin{aligned} P_{c_{i_{obj-obj}}} &= \frac{1}{2}\sigma_{obj} v_{r_i} n_{obj_i} (n_{obj_i} V_i - 1) \\ P_{c_{i_{obj-frag}}} &= \sigma_{obj} v_{r_i} n_{obj_i} n_{frag_i} V_i \end{aligned} \tag{4}$$

Two objects are removed for each impact within the intact objects family, which are all considered catastrophic, while collisions between intact objects and fragments are considered non-catastrophic. The corresponding number of particles added in the shell is computed from the NASA Standard Breakup Model formulas in [24], N_{nc} and N_c, for non-catastrophic and catastrophic impacts respectively.
The definition of a corrective factor to scale the overestimation of collisions cited in [12] is left for future work, along with a better distribution of the generated fragments in different altitude shells and inclusion of explosions.

3. The control

The possible control actions in Fig. 2 with which humans can influence the evolution of the objects' distribution in space are launch rate, post-mission disposals and active debris removals. In particular, previous works focused on efficient regulation of PMD compliance (e.g. [22]) and ADR rate (e.g. [11]). Given a constant maximum number of ADR per year, the time-varying percentage of removals term α is considered as input for the derivation of the control logic, which exploits a State-Dependent Differential Riccati Equations approach (SDDRE), but the same derivation applies to the other inputs, with appropriate modifications of the matrices. The feedback loop of the control action on the model is graphically represented in Fig. 3.

The system of ordinary differential Equations 3 is reformulated in state-space fashion (see Equation 5) and the resulting dynamics are time-varying and nonlinear in the state, due to the collision term. The state matrix is given by the sum of drag effect and collisions contributions, the former $\mathbf{F}_D$ in Equation 6 is only time-varying, the latter $\mathbf{F}_c$ in Equation 7 is also state-dependent. For the ADR controlled case considered, matrices $\mathbf{G}$ and $\mathbf{C}$ are defined as in Equations 8 and 9.

$$\dot{\mathbf{x}} = [\mathbf{F}_D + \mathbf{F}_c]\mathbf{x} + \mathbf{G}\mathbf{u} + \mathbf{C} \tag{5}$$

where:

$$\mathbf{x} = \begin{bmatrix} \mathbf{x}_{obj} \\ \mathbf{x}_{frag} \end{bmatrix}$$

$$\mathbf{F}_D = \begin{bmatrix} \mathbf{F_{D_{N_s}}} & \mathbf{0} \\ \mathbf{0} & \mathbf{F_{D_{N_s}}} \end{bmatrix} \tag{6}$$

$$\mathbf{F}_{D_{N_s}} = \begin{bmatrix} F_{D_{1,1}} & F_{D_{1,2}} & 0 & \dots & 0 \\ 0 & \ddots & \ddots & & \\ \vdots & & F_{D_{i,i}} & F_{D_{i,i+1}} & \\ & & & \ddots & \ddots \\ 0 & & & & F_{D_{N,N}} \end{bmatrix}$$

$$F_{D_{i,i}} = \frac{1}{V_i}(4\pi v_{r_i} r_{i_{lower}}^2)$$

$$F_{D_{i,i+1}} = -\frac{1}{V_i}(4\pi v_{r_{i+1}} r_{i_{upper}}^2)$$

$$\mathbf{F}_c = \begin{bmatrix} \mathbf{F_{c_{obj-obj}}} & \mathbf{0} \\ \mathbf{F_{c_{obj-frag}}} & \mathbf{0} \end{bmatrix} \tag{7}$$

$$\mathbf{F}_{c_{obj-obj}} = \begin{bmatrix} F_{o_{1,1}} & 0 & \dots & 0 \\ 0 & F_{o_{i,i}} & 0 & \dots \\ \vdots & & \ddots & \end{bmatrix}$$

$$F_{o_{i,i}} = -\frac{1}{V_i} v_{r_i} A_{obj}(x_i V_i - 1)$$

$$\mathbf{F}_{c_{obj-frag}} = \begin{bmatrix} F_{f_{1,1}} & 0 & \dots & 0 \\ 0 & F_{f_{i,i}} & 0 & \dots \\ \vdots & & \ddots & \end{bmatrix}$$

$$F_{f_{i,i}} = -A_{obj} v_{r_i} x_i + A_{obj} v_{r_i} x_i N_{nc} + A_{obj} v_{r_i} x_i N_c$$

$$\mathbf{G} = \begin{bmatrix} 0 & \dots & & 0 \\ \vdots & \ddots & & 0 \\ -G_1 & 0 & \dots & 0 \\ 0 & -G_i & 0 & \dots \\ \vdots & \dots & \ddots & \\ & \dots & & -G_{i_{N_{obj}}} \\ & \dots & \dots & 0 \\ 0 & \dots & \dots & \dots \end{bmatrix} \tag{8}$$

$$G_i = \frac{1}{V_i} \frac{N_{i_{ADR}}}{1year}$$

$$\mathbf{C} = \begin{bmatrix} C_1 \\ C_i \\ \vdots \end{bmatrix} \tag{9}$$

$$C_i = \frac{1}{V_i} \left(\frac{N_{i_L}}{1year} - \lambda \int_{V_{t_L}} \frac{\dot{n}_{i_L}(t_L)}{1year} \right)$$

Extending from previous work [14] a state-dependent optimal linear quadratic feedback controller is considered to tune the inputs. The method benefits from the extensively studied linear control techniques even in presence of state or control nonlinearities in the system.
The coefficient parametrisation in the state matrix $\mathbf{F}_c$ in Equation 5 is not unique, but this choice allows to correlate the different species through collisions, enforcing

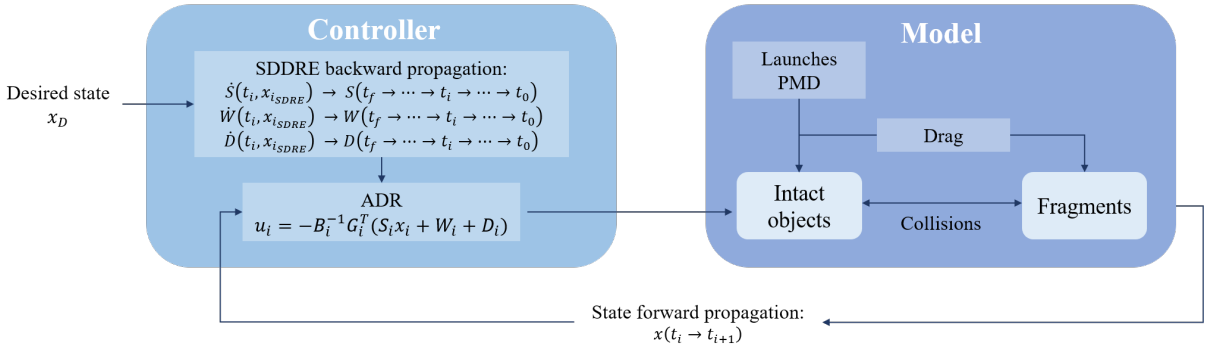

Fig. 3. Block scheme of the integrated system. In the model, the dynamics of intact objects and fragments is propagated at each time step under the effect of drag, launches, PMD, collisions and the controlled action of ADR. The feedback technique described in Section 3 is exploited in the control block to obtain the ADR removals based on the local error of the state at each time instant.

controllability of the system. The optimal control problem of the quasi-linear dynamics in Equation 5 is written as the minimisation of a quadratic cost function in the state error **e** with respect to a reference profile and control variables in Equation 10, in which weighting matrices **A** and **B** are positive definte and adequately chosen to bring the initial state to the final target scenario in a given time interval with acceptable levels of control and acceptable levels of the state [25].

$$J = \frac{1}{2}\mathbf{e}_f^T \mathbf{S}_f \mathbf{e}_f + \frac{1}{2}\int_{t_0}^{t_f} \left(\mathbf{e}^T \mathbf{A} \mathbf{e} + \mathbf{u}^T \mathbf{B} \mathbf{u}\right) dt \quad (10)$$

Applying the theory of calculus of variations and solving for the conditions of optimality, the control law in Equation 11 is derived, where **S** is a positive-definite matrix obtained solving the state-dependent differential optimal control Equation 12, which is an extension of the differential Riccati equation used in [14]. Moreover, to track a reference evolution $\mathbf{x}_d$ of the environment, matrix **W** is included in the control definition and since vector **C** in Equation 9 includes terms which do not depend on the state nor on the control inputs, they must be rejected as disturbances, which are launches and PMD in the ADR-controlled case. These effects are accounted for through the **D** matrix in Equation 11. **W** and **D** are obtained solving backward the differential Equations 13 and 14, which derive from the conditions of optimality [25][26][27]. A numerical approach is exploited to obtain the control matrices.

$$\mathbf{u} = -\mathbf{B}^{-1}\mathbf{G}^T(\mathbf{S}\mathbf{x} + \mathbf{W} + \mathbf{D}) \quad (11)$$

$$\begin{aligned} \dot{\mathbf{S}} =& -\mathbf{S}\mathbf{F} + \mathbf{S}\mathbf{G}\mathbf{B}^{-1}\mathbf{G}^T\mathbf{S} - \mathbf{A} - \mathbf{F}^T\mathbf{S} - \left(\frac{\partial \mathbf{F}}{\partial \mathbf{x}}\mathbf{x}\right)^T \mathbf{S} \\ & \mathbf{S}(t_f) = \mathbf{S}_f \end{aligned} \quad (12)$$

$$\begin{aligned} \dot{\mathbf{W}} =& \mathbf{S}\mathbf{G}\mathbf{B}^{-1}\mathbf{G}^T\mathbf{W} - \mathbf{F}^T\mathbf{W} + \mathbf{A}\mathbf{x}_d - \left(\frac{\partial \mathbf{F}}{\partial \mathbf{x}}\mathbf{x}\right)^T \mathbf{W} \\ & \mathbf{W}(t_f) = -\mathbf{S}_f \mathbf{x}_d \end{aligned} \quad (13)$$

$$\begin{aligned} \dot{\mathbf{D}} =& \mathbf{S}\mathbf{G}\mathbf{B}^{-1}\mathbf{G}^T\mathbf{D} - \mathbf{F}^T\mathbf{D} - \mathbf{S}\mathbf{C} - \left(\frac{\partial \mathbf{F}}{\partial \mathbf{x}}\mathbf{x}\right)^T \mathbf{D} \\ & \mathbf{D}(t_f) = \mathbf{0} \end{aligned} \quad (14)$$

The backpropagation of Equations 12-14 with final conditions is not straightforward, since it requires information of the state at future times, which is not available a priori. Different approaches have been proposed in literature for the solution of the nonlinear differential optimal control Equations 12-14: forward integration with frozen coefficients approximation [28], backward integration [26][27][29], solution of an approximated sequence of Riccati equations [28], state transition matrix solutions [26][29] and Lyapunov-based methods [26] [27] [28] [29]. The performance accuracy of backward integration techniques has been widely proven [29][28]. An auxiliary trajectory is used to obtain the state of the system at each backward step of the matrices' integration. As suggested in [26] [27] [28] [29] the sub-optimal State-Dependent Riccati Equations (SDRE) 15-17 are used as control logic to get the auxiliary trajectory, which are algebraic and where the derivative terms in the state have been discarded.

$$-\mathbf{S}\mathbf{F} + \mathbf{S}\mathbf{G}\mathbf{B}^{-1}\mathbf{G}^T\mathbf{S} - \mathbf{A} - \mathbf{F}^T\mathbf{S} = \mathbf{0} \quad (15)$$

$$\mathbf{S}\mathbf{G}\mathbf{B}^{-1}\mathbf{G}^T\mathbf{W} - \mathbf{F}^T\mathbf{W} + \mathbf{A}\mathbf{x}_d = \mathbf{0} \quad (16)$$

$$\mathbf{S}\mathbf{G}\mathbf{B}^{-1}\mathbf{G}^T\mathbf{D} - \mathbf{F}^T\mathbf{D} - \mathbf{S}\mathbf{C} = \mathbf{0} \quad (17)$$

Different methods have been studied in literature for solving the SDRE Equations, as the power-series approximation [26][30] and online numerical solution. The latter one is considered for the optimal gains derivation in GREEN SPECIES applying the Schur method [31]. Afterwards, matrices **S**, **W** and **D** are used in a forward propagation of the state under optimal control.
The SDDRE method allows systematic control of many

nonlinear dynamical systems, performing automatic analyses of different future evolutions of the debris environment. This is done in expense of some computational time than other faster but less-optimal controller designs, which is deemed acceptable since no online control of a real actuator is required in the GREEN SPECIES framework. Moreover, the method could be easily extended to account for control nonlinearities in non-affine systems, different cost functions and control approaches could be investigated changing Equation 10 and robust techniques could be combined with the SDDRE approach [26].

4. Analyses

Application of the controller described in Section 3 is now tested on different study cases. A common target is first defined and different controls to reach it within a 100 years period are analysed. The initial population is the one used in [22]. Only intact objects and fragments species are considered in the model of Section 2, so payloads, rocket bodies and large derelict objects are included in the former group, while fragments whose area is less than 1 m^2 define the second family. The launch traffic considered is a repetition of the yearly number of objects launched in the 5 years between 2017 and 2021, which are represented in Fig. 4. As an example of application of the methodology in Section 3, the target scenario is defined as a fixed profile of the number of objects in each shell. It is visible in Fig. 5 and it has been obtained limiting up to a maximum of 50% the increase in the number of intact objects and fragments in each shell after 100 years, when simulating the species evolution under the effect of drag and launches only (see Fig. 5). Other initial settings of the analysis are given in Table 1. The weight matrices of the cost function Equation 10 are constant, diagonal and definite positive, where each diagonal element is equal to $a_{i,i} = \frac{1}{t_f e^2_{i,i_{max}}}$ for the **A** matrix and $b_{i,i} = \frac{1}{t_f u^2_{i,i_{max}}}$ for the **B** matrix. The maximum acceptable absolute errors $e_{i,i_{max}}$ for intact objects and fragments in Table 1 have been set slightly different in order to account for the different orders of magnitude of the two contributions that enter the cost definition. The same weight $u_{i,i_{max}}$ has been applied to the different control actions considered.

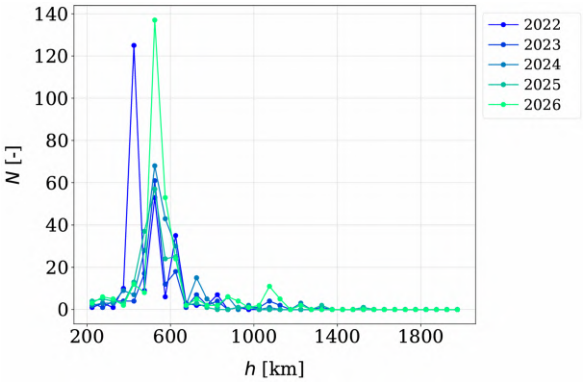

Fig. 4. Launch traffic profile from historical data, repeated every 5 years of the simulation.

Parameter	Common input	
t_f	100 years	
$e_{i,i_{max_{obj}}}$	$1 \times 10^{-18} m^{-3}$	
$e_{i,i_{max_{frag}}}$	$5 \times 10^{-18} m^{-3}$	
Parameter	Case 1	Case 2
u	λ	$[\lambda, \alpha]$
$u_{i,i_{max}}$	1	$[1, 1]$
λ		50%
$N_{i_{ADR}}$	$3\frac{\#}{year}$	$5\frac{\#}{year}$

Table 1. Simulation settings.

Two cases will be analysed, in the first only changes in the PMD compliance are inputs to the system, so the λ parameter in Equation 3 for each altitude shell, while the launch traffic in Fig. 4 is included as additional source. In the second case, the ADR percentage of a maximum number of 5 removals per year per shell is added as a control input, so the α parameter in Equation 3, leaving launches as source in the **C** matrix of Equation 5.

In Fig. 6 and 7 the resulting number of objects profiles per species is compared to the target one, the initial one and the only-launches scenario. The corresponding evolutions of the number of objects profiles are given in the same figures. The profiles in time of the relative errors with respect to the target are given in Fig. 8 and 9 for the two cases analysed. Finally, Fig. 10, 11 and 12 represent the control inputs evolution and cumulative action in time in each study. Fig. 10 is for PMD control only, and Fig. 11 and 12 are for the case with PMD and ADR control. The objects in the controlled space, from the shell including the 630 km re-entry limit on, appear mainly in two regions: between 1400 km and 1600 km and between 800 km and 1000 km. These regions will be considered separately to analyse the results.

Region 1: 1400-1600 km. Looking first at the objects' distribution between 1400 km and 1600 km, it is clear form Fig. 4 that no or few launches are performed there and consequently no PMD action is possible (see Fig. 10). In case 1, the final number of intact objects and fragments generated by collisions are equal to the only-launches scenario, since no mitigation is applied (see Fig. 6). In case 2 when the possibility of tuning ADR is available, more intact objects are removed between 1400 km and 1600 km (see Fig. 12), lowering the number of possibly colliding objects there and consequently the number of generated fragments (see Fig. 7). It must be considered that the target profiles in the number of

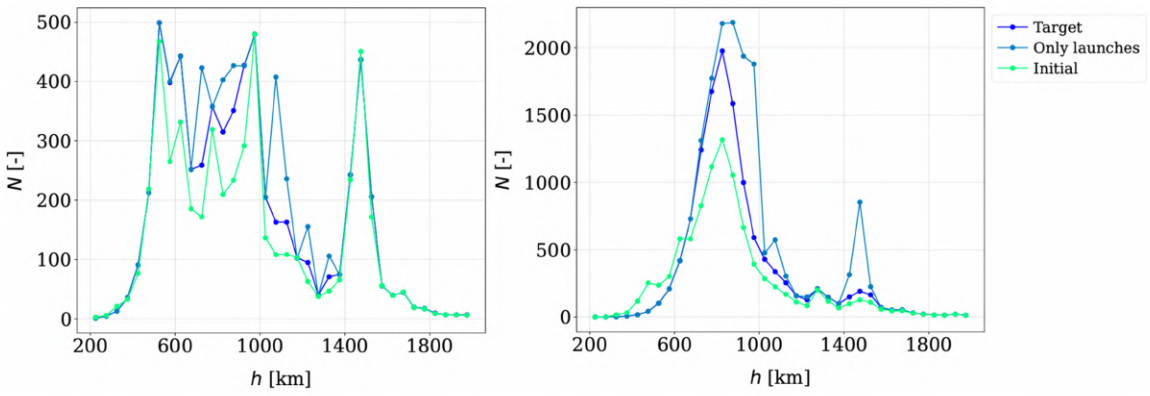

Fig. 5. Number of intact objects (left) and fragments (right) distributions: target scenario, only-launches simulation and initial population profile.

intact objects and in the number of fragments put contrasting objectives on the controller. In fact, in order to reduce the number of fragments it is necessary to reduce the number of intact objects and reduce collisions, however the desired number of objects is still close to the only-launches scenario. The control on ADR requires an initial large removal of intact objects, reaching saturation limit, to mitigate the fragments growth. When the error on the number of intact objects becomes predominant over the fragments one, no more ADR is performed and the number of fragments is allowed to increase mitigating the error on the number of objects (see Fig. 9). In case 2, the controller defines an equilibrium between the contrasting objectives given the weights provided and the limited control possibilities. In the results, no deposition effect of intact objects is actively controlled, such as the launch rate, so the requirement on their final number in this region cannot be met.

Region 2: 800-1000 km. Similarly to region 1, the target profiles in the number of intact objects and in the number of fragments put contrasting objectives on the controller. From the initial profile and the target distribution of intact objects in Fig. 5 it is possible to see how between 900 km and 1000 km the number of intact objects should be kept constant. In case 1, saturation of the control is required to act on the error in the number of fragments, causing an increasing error in the number of intact objects (see Fig. 8 and 10). However, even saturation of the control is not sufficient to limit the growth of fragments. Similarly in the lower shells, the number of objects is first reduced through saturation of PMD compliance, increasing the relative error of this species' profile in the region, but keeping the evolution of the number of fragments close to the target shape. Then, both families are allowed to grow in number to try and match the final desired distribution, reducing the relative errors with no control action needed (see Fig. 6 and 10). ADR is exploited in case 2 to reduce more the number of intact objects between 900 km and 1000 km causing a limited growth in the number of fragments at the beginning of the simulation, this allows to limit the final error on the fragments, that increases again when the error in the intact objects contribution becomes dominant, in expense of a slightly worse final result of the intact objects than case 1 (see Fig. 9, 11, 12). Below 900 km, the combined inputs act to change the distribution of intact objects, in order to control indirectly the profile of the fragments and keep both relative errors low. The numbers of the two species are allowed to increase as targeted but in a controlled way, so as to progressively approach the final profile in the simulation time given. ADR control takes on most of the mitigation action, reducing much the PMD required with respect to case 1. In case 2 PMD is saturated only at the end, when the controller tries to get closer to the final target (see Fig. 11). Saturation of ADR up to 5 removals per year is reached only at the initial years of the simulations (see Fig. 12). Still, not all the requirements in terms of final objects and fragments values in each shell can be met, but a balance between contrasting objectives is enforced.

When more flexibility on the input action is given to the controller it defines a more efficient strategy to approach the target scenarios, with contrasting objectives for intact objects and fragments, given the weights provided. This highlights the effects reachable with limited control. Separate weights for state and inputs have a strong influence on the criteria for strategy selection and many more scenarios can be investigated by changing them. Different inputs can be considered singularly or combined, and different costs of their implementation accounted for in the control objective.

5. Conclusions and future work

Debris proliferation can be considered as an environmental stressor of Earth's orbital environment. As such, its studying and mitigation activities follow the same scientific approach of other climate phenomena. Taking example from the widely spread and recognised re-

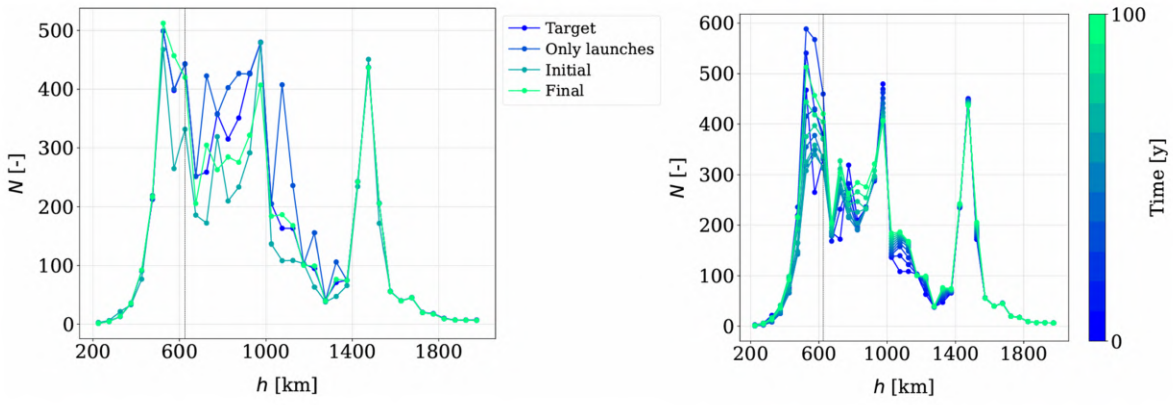

(a) Case 1 - Left: final distribution of the number of intact objects compared with the profiles of Fig. 5. Right: evolution over time of the number of intact objects distribution. The vertical dotted line defines the limit of the control action for PMD.

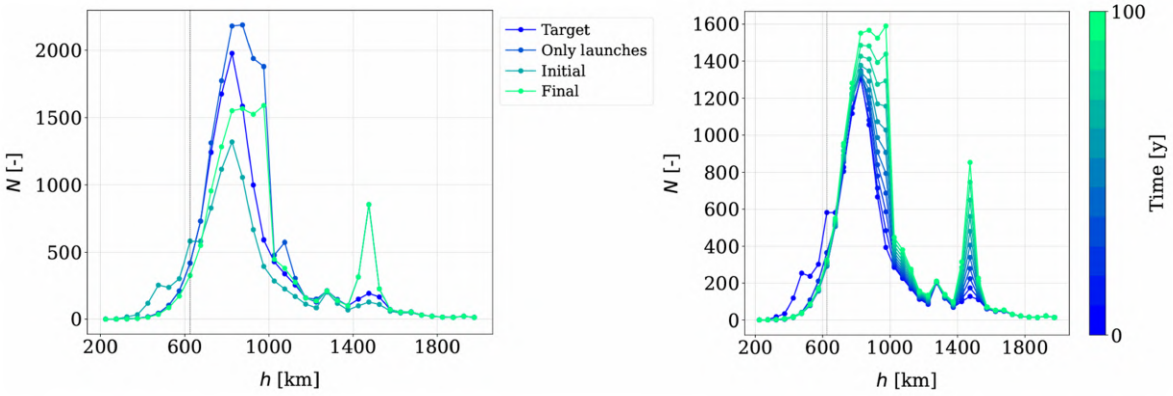

(b) Case 1 - Left: final distribution of the number of fragments compared with the profiles of Fig. 5. Right: evolution over time of the number of fragments distribution. The vertical dotted line defines the limit of the control action for PMD.

Fig. 6. Case 1 - Resulting number of objects distribution of the two species, final profile and evolution in time.

search in integrated assessment models of climate economics, the GREEN SPECIES project aims at developing a socio-economic controlled system of the space debris environment. Currently, a statistical one-dimensional model in orbital radius is considered to predict the future evolution of the spatial density of objects, in each altitude shell in which the domain is divided. In the modelled dynamics, intact objects and smaller fragments' distribution evolve under the effect of atmospheric drag, launches, post-mission disposals, active debris removals and in-orbit collisions. A state-dependent linear feedback controller is applied to the system to tune inputs and reach a desired target scenario minimising a quadratic cost function. Different contributions can act as control inputs, separately or combined: launch rate, post-mission disposal compliance and active debris removal rate. The SDDRE method allows systematic control of many nonlinear dynamical systems. Two application cases showed the capability of the controller to deal with contrasting objectives reaching a balanced final result. Combination of ADR input with PMD compliance input in case 2 of Section 4 provides a beneficial larger flexibility in the control action.

The system's capability to represent a realistic evolution of the environment of orbiting objects is still limited. Actions for future work include: addition of explosions to the model and investigation of different profiles for launch traffic and ADR. Study of the versatility and wide range of application of the actively controlled system has just started. Different control logics will be tested in future developments of the project, with both continuous and discrete approaches. Different inputs combinations and cost functions definition will also be considered.

Acknowledgements

The research received funding from the European Research Council (ERC) under the European Union's Horizon Europe research and innovation program as part of the GREEN SPECIES project (Grant agreement No - 101089265). The simulations have been performed using as reference population the data in [22], kindly pro-

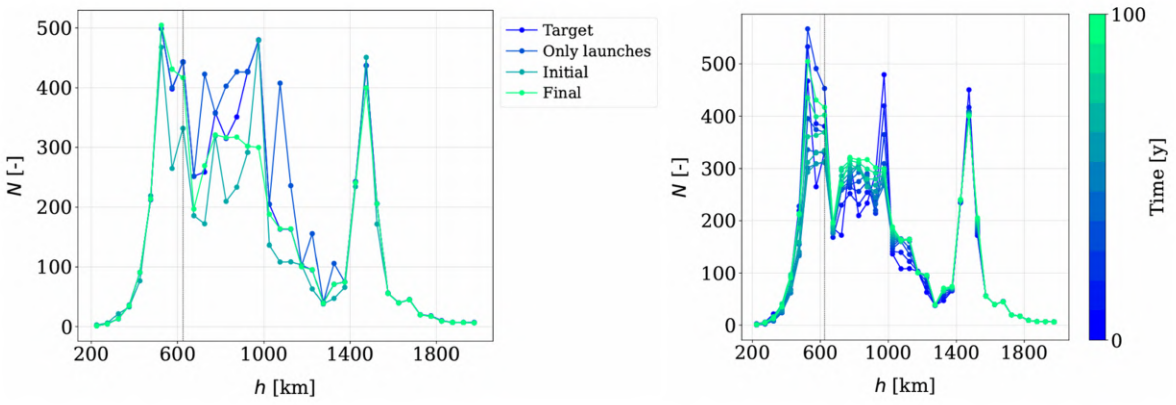

(a) Case 2 - Left: final distribution of the number of intact objects compared with the profiles of Fig. 5. Right: evolution over time of the number of intact objects distribution. The vertical dotted line defines the limit of the control action for PMD and ADR.

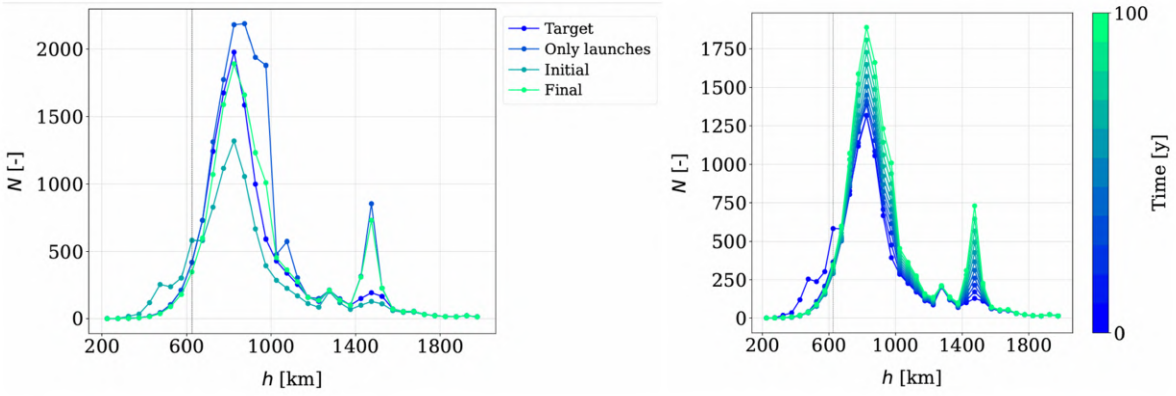

(b) Case 2 - Left: final distribution of the number of fragments compared with the profiles of Fig. 5. Right: evolution over time of the number of fragments distribution. The vertical dotted line defines the limit of the control action for PMD and ADR.

Fig. 7. Case 2 - Resulting number of objects distribution of the two species, final profile and evolution in time.

vided by the European Space Agency.

References

[1] ESA Space Debris Office, "Esa's annual environment report," European Space Agency, Tech. Rep., 2023.

[2] D. L. Talent, "Analytic model for orbital debris environmental management," *Journal of Spacecraft and Rockets*, vol. 29, no. 4, pp. 508–513, 1992. doi: 10.2514/3.25493.

[3] A. Rossi, L. Anselmo, A. Cordelli, P. Farinella, and C. Pardini, "Modelling the evolution of the space debris population," *Planetary and Space Science*, vol. 46, no. 11, pp. 1583–1596, 1998. doi: 10.1016/S0032-0633(98)00070-1.

[4] L. Giudici, C. Colombo, A. Horstmann, F. Letizia, and S. Lemmens, "Density-based evolutionary model of the space debris environment in low-earth orbit," *Acta Astronautica*, vol. 219, pp. 115–127, 2024. doi: 10.1016/j.actaastro.2024.03.008.

[5] IADC Steering Group and Working Group 4, "Iadc space debris mitigation guidelines," Inter-Agency Space Debris Coordination Committee, Tech. Rep., 2021.

[6] ESA Space Debris Mitigation Working Group, "Esa space debris mitigation requirements," European Space Agency, Tech. Rep., 2023.

[7] W. Nordhaus, "Chapter 16 - integrated economic and climate modeling," in *Handbook of Computable General Equilibrium Modeling SET, Vols. 1A and 1B*, ser. Handbook of Computable General Equilibrium Modeling, P. B. Dixon and D. W. Jorgenson, Eds., vol. 1, Elsevier, 2013, pp. 1069–1131. doi: 10.1016/B978-0-444-59568-3.00016-X.

[8] H. Lewis, G. Swinerd, R. Newland, and A. Saunders, "The fast debris evolution model," *Advances in Space Research*, vol. 44, no. 5, pp. 568–578, 2009. doi: 10.1016/j.asr.2009.05.018.

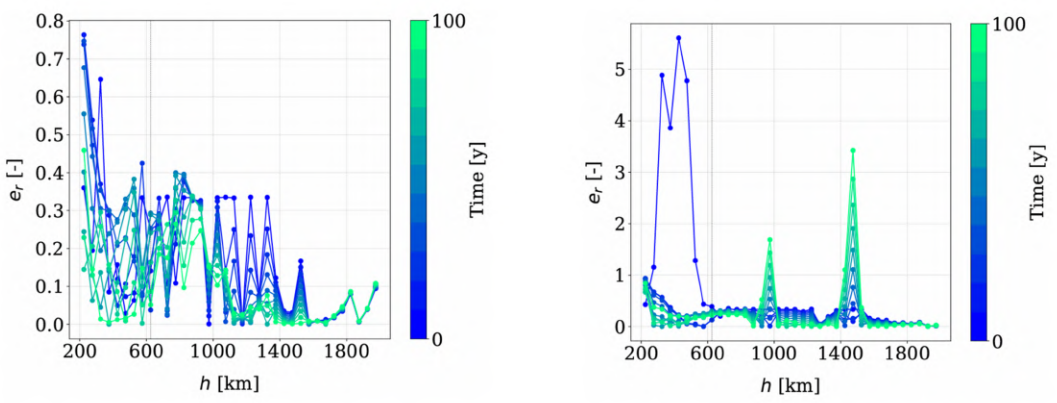

Fig. 8. Case 1 - Left: evolution in time of the relative error between the distribution of the number of intact objects and the target profile. Right: evolution in time of the relative error between the distribution of the number of fragments and the target profile. The vertical dotted line defines the limit of the control action for PMD.

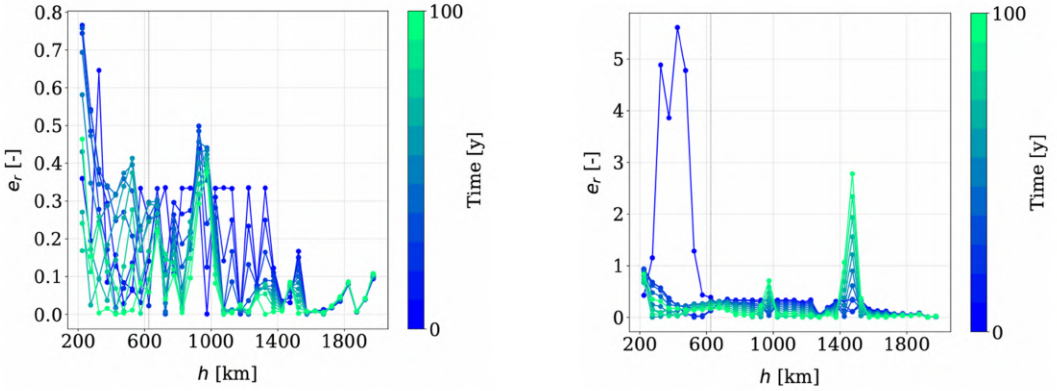

Fig. 9. Case 2 - Left: evolution in time of the relative error between the distribution of the number of intact objects and the target profile. Right: evolution in time of the relative error between the distribution of the number of fragments and the target profile. The vertical dotted line defines the limit of the control action for PMD and ADR.

[9] D. Finkleman, "Debris removal to reduce risk," in *52nd Aerospace Sciences Meeting*. doi: 10.2514/6.2014-0301.

[10] P. Farinella and A. Cordelli, "The proliferation of orbiting fragments: A simple mathematical model," *Science & Global Security*, vol. 2, no. 4, pp. 365–378, 1991. doi: 10.1080/08929889108426373.

[11] A. E. White and H. G. Lewis, "An adaptive strategy for active debris removal," *Advances in Space Research*, vol. 53, no. 8, pp. 1195–1206, 2014. doi: 10.1016/j.asr.2014.01.021.

[12] G. L. Somma and Supervisors: H. Lewis and - C. Colombo, "Adaptive remediation of the space debris environment using feedback control," Ph.D. dissertation, Jul. 2019. [Online]. Available: https://eprints.soton.ac.uk/447843/.

[13] R. Mia Tian, K. Xi, G. Lavezzi, M. Lifson, S. Servadio, and R. Linares, "Optimizing active debris removal strategies with feedback control for a sustainable space environment," in *Astrodynamics Specialist Conference*, 2024.

[14] M. Rusconi and C. Colombo, "Active feedback control on post-mission disposal compliance to limit the space debris proliferation," in *In proceedings of the 29th International Symposium on Space Flight Dynamics*, 2024.

[15] D. J. Kessler, "Derivation of the collision probability between orbiting objects: The lifetimes of jupiter's outer moons," *Icarus*, vol. 48, no. 1, 39 bibrangedash 48, 1981. doi: 10.1016/0019-1035(81)90151-2.

[16] C. McInnes, "Simple analytic model of the long-term evolution of nanosatellite constellations," *Journal of Guidance Control and Dynamics*, vol. 23, Mar. 2000. doi: 10.2514/2.4527.

[17] F. Letizia and Supervisors: C. Colombo and H. Lewis, "Space debris cloud evolution in low earth

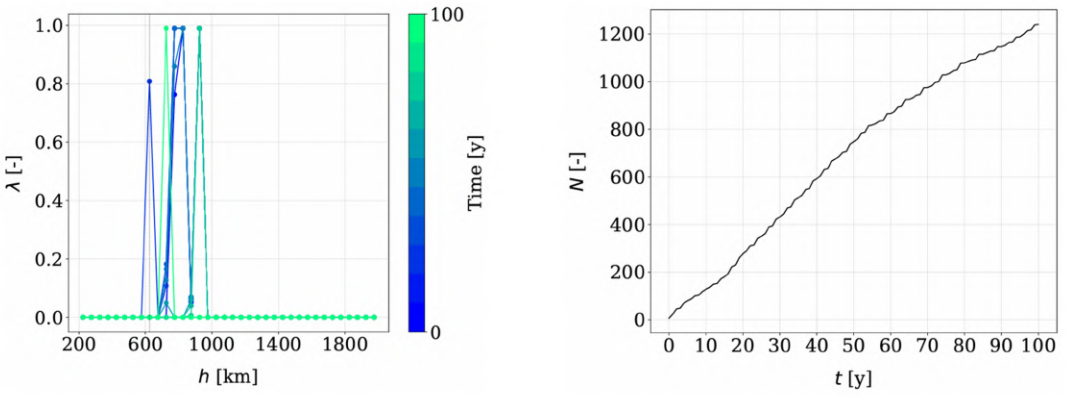

Fig. 10. Case 1 - Left: evolution in time of the PMD compliance acting on the intact objects population. Right: cumulative number of PMD opearions obtained. The vertical dotted line defines the limit of the control action for PMD.

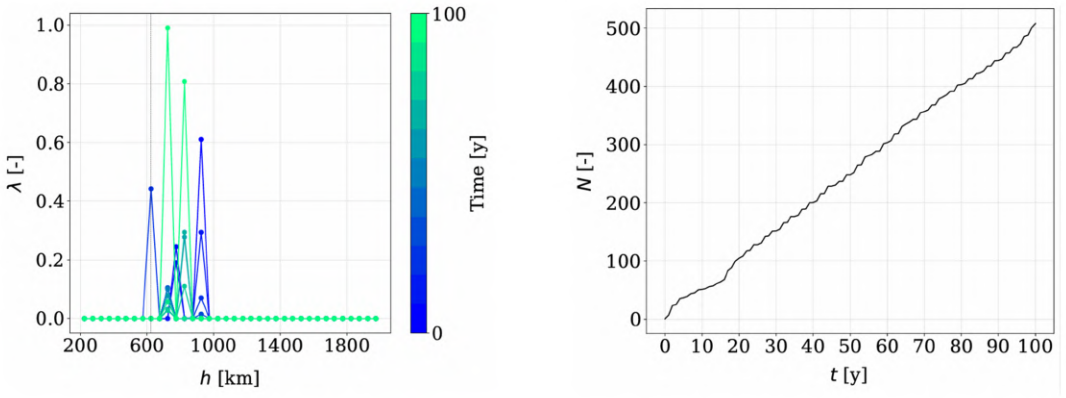

Fig. 11. Case 2 - Left: evolution in time of the PMD compliance acting on the intact objects population. Right: cumulative number of PMD opearions obtained in all the shells. The vertical dotted line defines the limit of the control action for PMD and ADR.

orbit," Ph.D. dissertation, Feb. 2016. doi: 10.13140/RG.2.1.3817.7047.

[18] C. Colombo, F. Letizia, and H. Lewis, "Spatial density approach for modelling of the space debris population," in *AAS/AIAA Space Flight Mechanics Meeting*, Feb. 2016.

[19] C. Duran, L. Giudici, and C. Colombo, "Modelling the whole space debris environment through a spatial density approach," in *AAS/AIAA Astrodynamics Specialist Conference*, Aug. 2021.

[20] S. Frey, C. Colombo, and S. Lemmens, "Application of density-based propagation to fragment clouds using the starling suite," in *First International Orbital Debris Conference*, Dec. 2019.

[21] D. G. King-Hele., *Theory of Satellite Orbits in an Atmosphere*. Butterworths Mathematical Texts, 1964. doi: 10.1002/qj.49709038627.

[22] F. Letizia, B. Bastida Virgili, and S. Lemmens, "Assessment of orbital capacity thresholds through long-term simulations of the debris environment," *Advances in Space Research*, vol. 72, no. 7, pp. 2552–2569, 2023. doi: 10.1016/j.asr.2022.06.010.

[23] D. Kessler, N. Johnson, J.-C. Liou, and M. Matney, "The kessler syndrome: Implications to future space operations," in *Rocky Mountain Guidance and Control Conference, Advances in the Astronomical Sciences*, vol. 137, 2010, pp. 47–62.

[24] N. Johnson, P. Krisko, J.-C. Liou, and P. Anz-Meador, "Nasa's new breakup model of evolve 4.0," *Advances in Space Research*, vol. 28, no. 9, pp. 1377–1384, 2001. doi: 10.1016/S0273-1177(01)00423-9.

[25] A. E. Bryson, Y.-C. Ho, and G. M. Siouris, "Applied optimal control: Optimization, estimation, and control," *IEEE Transactions on Systems, Man, and Cybernetics*, vol. 9, no. 6, pp. 366–367, 1979. doi: 10.1109/TSMC.1979.4310229.

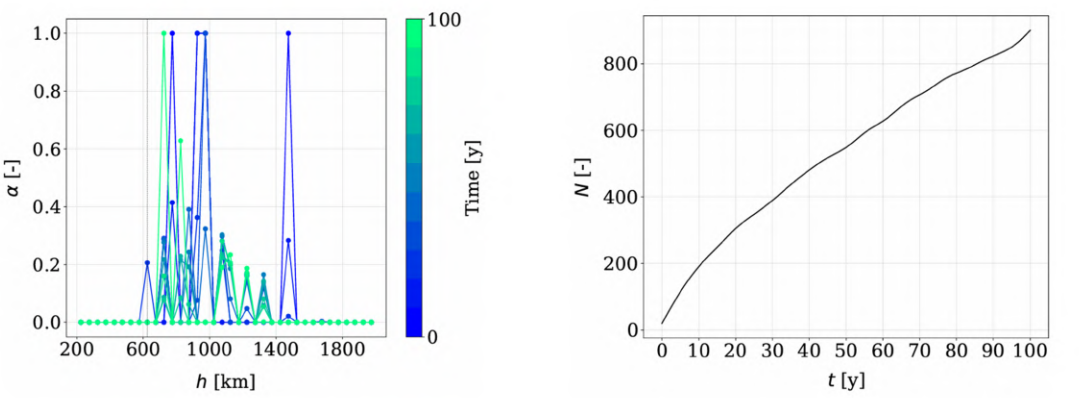

Fig. 12. Case 2 - Left: evolution in time of the ADR percentage of maximum removals acting on the intact objects population. Right: cumulative number of ADR opearions obtained in all the shells. The vertical dotted line defines the limit of the control action for PMD and ADR.

[26] S. R. Nekoo, "Tutorial and review on the state-dependent riccati equation," *Journal of Applied Nonlinear Dynamics*, vol. 8, pp. 109–166, Jun. 2019. doi: 10.5890/JAND.2019.06.001.

[27] M. H. Korayem and S. R. Nekoo, "State-dependent differential riccati equation to track control of time-varying systems with state and control nonlinearities," *ISA Transactions*, vol. 57, pp. 117–135, 2015. doi: 10.1016/j.isatra.2015.02.008.

[28] A. A. Kabanov, "Finite-time state-dependent coefficient method for optimal control of nonlinear systems," in *International Conference on Industrial Engineering, Applications and Manufacturing (ICIEAM)*, 2022, pp. 717–721. doi: 10.1109/ICIEAM54945.2022.9787138.

[29] M. H. Korayem and S. R. Nekoo, "Finite-time state-dependent riccati equation for time-varying nonaffine systems: Rigid and flexible joint manipulator control," *ISA Transactions*, vol. 54, pp. 125–144, 2015. doi: 10.1016/j.isatra.2014.06.006.

[30] S. Beeler and D. Cox, "State-dependent riccati equation regulation of systems with state and control nonlinearities," Tech. Rep., Aug. 2004.

[31] A. Laub, "A schur method for solving algebraic riccati equations," *IEEE Transactions on Automatic Control*, vol. 24, no. 6, pp. 913–921, 1979. doi: 10.1109/TAC.1979.1102178.